AIAA '89

AIAA 89-0845
Interaction of Vortex Ring with a Density Interface

C. Schneil and W. Dahm, Univ. of Michigan, Ann Arbor, MI

27th Aerospace Sciences Meeting

January 9–12, 1989/Reno, Nevada

AIAA-89-0845

INTERACTION OF A VORTEX RING WITH A DENSITY INTERFACE

Christine Scheil, Prof. W.J.A. Dahm
University of Michigan
Department of Aerospace Engineering
Ann Arbor, Michigan 48109

Abstract

We present results from an experimental investigation into the dynamics of a thin-cored vortex ring with diameter a and circulation Γ encountering a planar interface of thickness δ across which the density increases from ρ_1 to ρ_2. When $\delta << a$ and $(a^3 g/\Gamma^2) >> 1$, the interaction should be determined by a single parameter, namely $[(\rho_1-\rho_2)/(\rho_1+\rho_2)](a^3 g/\Gamma^2)$. This has been verified by our experiments. Results show that the vortex can penetrate the interface and subsequently mix the fluids only when this parameter exceeds a critical value. It also appears that baroclinically generated vorticity from the interface plays the dominant role in the dynamics of the interaction, with such rings displaying a Widnall-like instability modified by the presence of extensional or compressional azimuthal strain.

Nomenclature

a	ring diameter
g	gravity
P	pressure
t	time
u	velocity
δ	interface thickness
Γ	ring circulation
ρ_1	density of fluid 1
ρ_2	density of fluid 2
ν	kinematic viscosity
ω	vorticity
D( )/Dt	Lagrangian derivative
∇	gradient operator
( )'	dimensionless quantity

Introduction

The study of turbulence is currently receiving a great deal of attention, due to the relative lack of knowledge of the complex interactions occuring in a turbulent flow field. An interesting aspect of this field of study is the interaction of turbulence with a density inhomogeneity. This type of interaction has a wide range of applications, for example: in combustion, fuel injected into oxidizer of different density; in atmospheric studies, thermals rising into a stratified atmosphere; general problems of two-fluid mixing; ships' turbulent wakes interacting with the ocean surface; shock wave interaction with a fluid bubble; as well as various aerodynamic applications.

Vorticity in general is difficult to study due to the complexity of the flow field, and the resulting inability to resolve interactions. Therefore, we chose to study a comparatively simple vorticity field, the vortex ring. The structure and motion of such vortex rings, as well as their stability characteristics, have been studied for many years,[1,2,3,4] thus making them a favorable choice for the study of vorticity interaction with a density inhomogeneity. The simplest density inhomogeneity that can be studied is a planar density interface. Linden[5] has examined the interaction of a turbulent vortex ring with a planar density interface. However, the emphasis of that experiment was quite different from that considered here, and provided no detailed information about the dynamics of the interaction. In this paper, we examine the interaction of an incompressible laminar vortex ring with a planar density interface in a relatively simple experiment designed to yield important basic results applicable to many types of more complex flows.

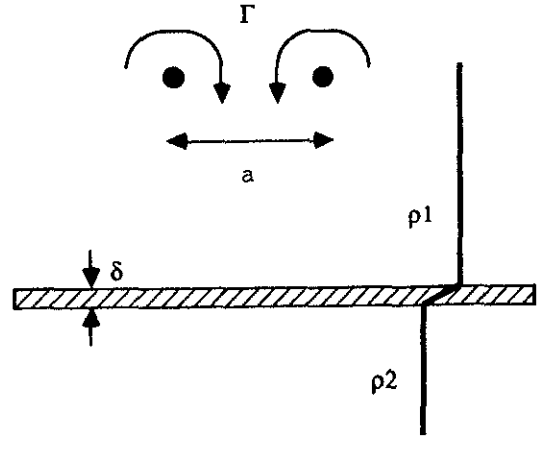

Figure 1. Diagram of relevant parameters.

Theoretical Considerations

This experiment deals with the behavior of a thin-cored vortex ring of diameter a and circulation Γ encountering a density interface of thickness δ, across which the density increases from ρ_1 to ρ_2 (see Fig. 1).

In analyzing the motion of vortex rings, we began with the vorticity transport equation, nondimensionalized it, and identified

*Graduate student, Dept. of Aerospace Engineering
Student Member AIAA

the important parameters governing the dynamics of their interaction with a density interface. The vorticity transport equation is made up of the following terms:

$$\underset{\text{change in vorticity}}{D\omega/Dt} = \underset{\text{vortex line stretching}}{(\omega \cdot \nabla)u} - \underset{\text{baroclinic generation of vorticity}}{(1/\rho^2)(\nabla\rho \times \nabla P)} + \underset{\text{diffusion of vorticity}}{\nu\nabla^2\omega} + \underset{\text{=0 by cons. of mass}}{\omega(\nabla \cdot u)} \quad (1)$$

To make the results applicable to many different ring cases, ω, u, t, x, P, and ρ were nondimensionalized by appropriate combinations of the ring circulation Γ and ring diameter a; for example, $t' = t/(a^2/\Gamma)$. The density ρ is replaced with $(\rho_1 + \rho_2)$. We consider separately the contributions from the hydrostatic pressure and the hydrodynamic pressure. Nondimensionalizing, the pressure gradient terms become:

$$\text{hydrostatic: } \nabla P_{hs} = (\rho_1 + \rho_2) g \nabla P'_{hs}$$

$$\text{hydrodynamic: } \nabla P_{hd} = (\rho_1 + \rho_2)(\Gamma^2/a^3)\nabla P'_{hd}$$

When all the dimensionless quantities are substituted into the vorticity transport equation, the following dimensionless form is obtained:

$$D\omega'/Dt = (\omega' \cdot \nabla)u' - [(\rho_1-\rho_2)/(\rho_1+\rho_2)](a^3g/\Gamma^2)(a/\delta)\nabla\rho' \times \nabla P'_{hs} - [(\rho_1-\rho_2)/(\rho_1+\rho_2)](a/\delta)\nabla\rho' \times \nabla P'_{hd} + (\nu/\Gamma)\nabla^2\omega' \quad (2)$$

The original hypothesis was that for (Γ/ν) large, i.e., $Re >> 1$, (δ/a) small, i.e., a thin interface, and (a^3g/Γ^2) large, i.e., the hydrostatic term much larger than the hydrodynamic term, the coefficient $[(\rho_1-\rho_2)/(\rho_1+\rho_2)](a^3g/\Gamma^2)$ is the important matching parameter for a vortex ring hitting a density interface. This parameter can be thought of as either a dimensionless interface strength or the inverse of a dimensionless vortex strength, and will henceforth be referred to simply as the vortex strength. One of the goals of this experiment was to investigate the hypothesis that, if the value of this vortex strength were held fixed and density ratio and ring circulation varied appropriately, the behavior of the vortex ring would remain the same. Since the dynamics of a free vortex ring are strongly dependent on the core radius, the precise numerical values obtained from our experiments must be viewed as being specifically for our configuration. However, the features associated with the dynamics of the interaction will likely apply to the entire class of such problems.

Experimental Apparatus

The vortex rings are created when a strictly regulated pulse of high-pressure air forces a 'blob' of fluid out of a nozzle into a tank of water; as the fluid flows out of the nozzle, it rolls up into a vortex ring. An air-driven system was chosen over the more conventional piston-driven system due to the inherent instabilities of the piston system; i.e., any vibrations in the piston mechanism propagate into the ring fluid, thus causing unstable rings to form. With the air-driven system, we are able to create very sharp, 'clean' rings.

The complete drive system (see Fig. 2a.) consists of the following components:

1. compressed air tank
2. regulator set at 60 psi.
3. pressure vessel pressurized to 60 psi.: provides a large source of high-pressure air that can be drawn upon when a ring is being created.
4. ON/OFF solenoid valve: turns flow of air on or off
5. sonic metering valve: controls air mass flow; its throat is the smallest area point in the system and allows accurate regulation of air mass flow
6. fluid-mechanical low-pass filter: consists of a 'capacitor/resistor' in parallel which filters out high frequencies in the pressure pulse to avoid exciting the natural frequency of the system, causing unstable rings
7. timer box: regulates length of pressure pulse; typically set for approximately 200ms.
8. plenum and nozzle: made of lucite and filled with dyed water from which the ring is created

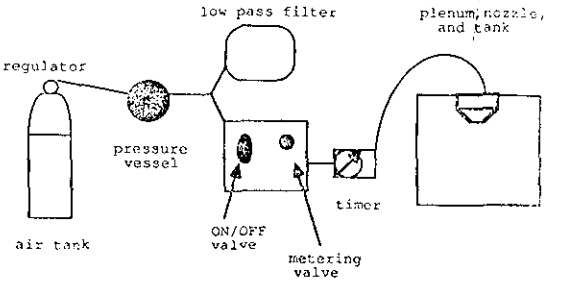

Figure 2a. Experimental apparatus

Figure 2b. Nozzle, plenum, and typical vortex ring

The nozzle exit has a diameter of 3.9cm., producing a ring with a diameter of 4.9cm., and ring core diameter estimated to be approximately 5mm. The variability of this drive system allows the production of rings of widely varying circulation, or strength. The accuracy of the metering valve and timer box allow for repeatability of all ring types. A typical vortex ring produced by this system can be seen in Figure 2b.

The tank itself is approximately one foot square. The bottom half of the tank is filled with water mixed with either salt or glycerine to make it heavier than the top layer of fresh water. The density of the bottom fluid ranges from 0.2% to 3% greater than the density of the top fluid layer. To set up the interface between these two density layers, a water-soaked piece of foam rubber is placed on top of the heavy fluid, and fresh water is slowly poured onto it. As the tank fills, the foam floats to the top and is then carefully removed, leaving behind two distinct layers of fluid.

The vortex ring motion is made visible by dying both the ring itself and the heavy fluid with either food coloring or laser dyes. The food coloring allows visualization of the three-dimensional ring. The laser dyes are used in conjunction with a 5.5W Argon-ion laser, which is set up such that a thin sheet of laser light slices through the center of the tank and the ring. Using laser-induced fluorescence (LIF) allows better visualization of the internal behavior of the ring upon its interaction with the density interface. The ring motion is recorded by either a high speed movie camera or a 35mm Nikon camera.

The displacement of the freesurface in the plenum was measured with the movie camera. Once this freesurface velocity was known, it was possible to estimate from this the resulting ring circulation. Ring circulation varies from 20cm^2/s to 160cm^2/s. A problem with firing rings of large circulation is that a secondary ring is produced that travels downward and can interfere with the interaction of the original ring with the density interface, although this interference usually occurs late enough that the important aspects of the interaction can be accurately observed.

Experimental Results

This experiment dealing with the interaction of a laminar vortex ring with a density interface has yielded a number of important results, including, proof of the governing matching parameter, the first documentation of this type of interaction, and data on depth of ring penetration.

Proof of Similarity

By experiment, we have proven that the parameter obtained in nondimensionalizing the vorticity transport equation,

$$[(\rho_1-\rho_2)/(\rho_1+\rho_2)](a^3g/\Gamma^2)$$

the vortex strength, is the important matching parameter for this interaction. Holding the value for the vortex strength fixed, the values for ring circulation and density ratio were varied appropriately, and it was found that the rings created in each case had the same behavior. Figure 3 show a comparison of two weak ring cases, both with vortex strength of 1.20. (Note: s.g.= specific gravity). Figures 3a. and 3b. show a ring with circulation Γ = 38.1cm^2/s and density interface with specific gravity of 1.028, i.e., ρ_2 is 2.8% greater than ρ_1. Figures 3c. and 3d. show a ring with Γ = 22.2cm^2/s and specific gravity of 1.01. (Note: the straight line appearing in the photos is attached to the back of the tank, and indicates the initial position of the density interface.) As can be seen from these photographs, the ring behavior upon encountering the interface is essentially the same.

Figure 4 shows a comparison between two strong ring cases, with the value of the vortex strength equal to 0.025. Figures 4a. and 4b. show a ring with Γ = 107cm^2/s and specific gravity of 1.005. The photographs shown in 4a. and 4b. were obtained using laser-induced fluorescence, and show the internal structure of the ring. Figures 4c. and 4d. show a ring with Γ = 154cm^2/s and specific gravity of 1.01. Again it is apparent that the ring behavior for these two widely varying sets of conditions is the same. With these experiments, we have shown that given the value for

$$[(\rho_1-\rho_2)/(\rho_1+\rho_2)](a^3g/\Gamma^2)$$

it is possible to predict the behavior of a ring encountering a density interface, regardless of the ring circulation and strength of the interface.

Photographic Results

This experiment has also documented the detailed dynamics resulting from the interaction of a vortex ring with a density interface, important results that can be applied to the more general problem of vorticity interaction, with density inhomogeneities. Figures 5 through 8 are photographs of ring cases ranging from interaction at a solid wall to a strong ring case where the ring will penetrate through the interface.

Figure 5 shows a ring hitting a solid wall - which might be thought of as an infinite density interface. The photos are simultaneous bottom and side views of the ring obtained by the use of a mirror set at 45° beneath the tank. Note the formation of a secondary and tertiary ring of opposite circulation to the original ring. These rings are formed because of the no-slip condition at the wall. Note also the Widnall-like wavy instability that occurs when the secondary ring is drawn into the primary ring.

Figures 6 through 8 are for various ring cases with a density interface set up in the tank. Figure 6 is a weak ring/strong interface (ring of low circulation/large density change). Figure 7 is an intermediate case, and figure 8 is a strong ring/weak interface case done with LIF. As the value for the vortex strength grows progressively smaller, the ring is able to penetrate the interface more deeply. In each of these cases, secondary and tertiary rings of opposite circulation of the primary ring form due to baroclinic generation of vorticity at the density interface (see figures 6e., 7e., 8f. for formation of the

secondary ring). As this secondary ring is drawn into, or orbits around, the primary ring, its diameter decreases and it undergoes compressional strain, resulting in the formation of waves of instability. The primary ring diameter increases when it strikes the interface, and it experiences a stabilizing extensional strain.

It is interesting to note the similarity between the solid wall case and the weak ring/strong interface cases; the ring behavior in the two cases appears to be qualitatively the same. Because of this similarity, it is suspected that the two cases can be related, and this possibility is currently being studied.

Depth of Penetration

By experiment, it has been found that there appears to be a critical value for

$$[(\rho_1-\rho_2)/(\rho_1+\rho_2)](a^3 g/\Gamma^2)$$

above which the ring is unable to penetrate the interface. Figure 9 is a plot of depth of penetration normalized by ring diameter vs. the inverse of the dimensionless vortex strength. It is clear from the plot that for values of the vortex strength above approximately 0.5, the ring can penetrate the interface only a minimal amount. Below this value, the depth of penetration increases rapidly with a small change in the value of the vortex strength.

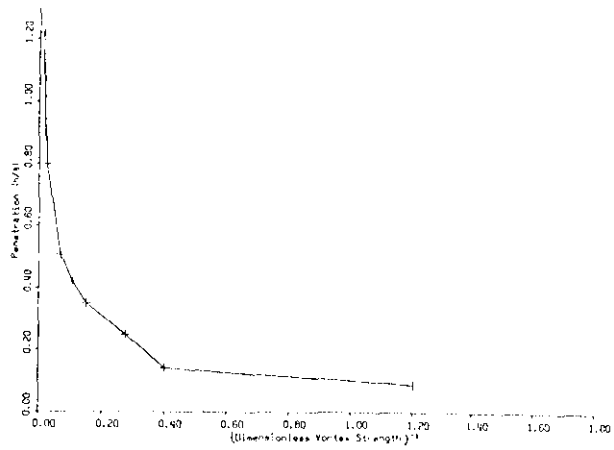

Figure 9. Normalized depth of penetration vs. inverse dimensionless vortex strength.

Conclusions

The study of vortex motion is currently very popular due to its wide range of applications. In particular, the interaction of vorticity with a density inhomogeneity, in the form of a vortex ring hitting a planar density interface, is of great interest. Our experiment has provided the first documentation of this type of interaction, it has allowed the identification of the important matching parameter, the inverse of the dimensionless vortex strength , and has provided data on the ring's depth of penetration under various conditions. Although the experiment itself is relatively simple to perform, the results it has yielded are applicable to a wide range of more complex flows.

References

1. Krutzsch, C.H., "Uber Eine Experimentell Beobachtete Erscheinung an Wirbelringen bei Translatorischen Bewegung in Wirklichen Flussigkeiten", Annalen der Physik, 5.Folge, Band 35, 1939, pp. 497-522.

2. Saffman, P.G., "The Velocity of Viscous Vortex Rings", Studies in Applied Mathematics, vol. XLIX no.4, Dec. 1970, pp.371-380.

3. Maxworthy, T., "The Structure and Stability of Vortex Rings", Journal of Fluid Mechanics, vol.51, part 1, 1972, pp. 15-32.

4. Widnall, S.E. and Sullivan, J.P., "On the Stability of Vortex Rings", Proceedings of the Royal Society, London, A. 332, 1973, pp.335-353

5. Linden, P.F., "The Interaction of a Vortex Ring with a Sharp Density Interface: a Model for Turbulent Entrainment', Journal of Fluid Mechanics, vol.60 part3, 1973, pp.467-480.

6. Saffman, P.G., "The Number of Waves on Unstable Vortex Rings", Journal of Fluid Mechanics, vol.84 part 4, 1978, pp. 625-639.

7. Walker, J.D.A. and Smith, C.R., "The Impact of a Vortex Ring on a Wall", Journal of Fluid Mechanics, vol.181, 1987, pp. 90-140.

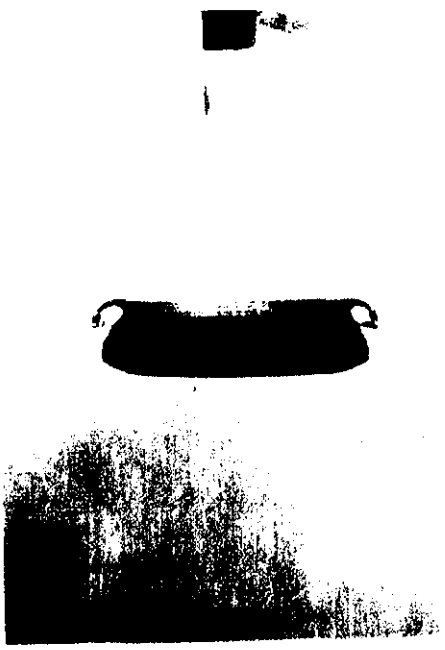

3a.

3c.

3b.

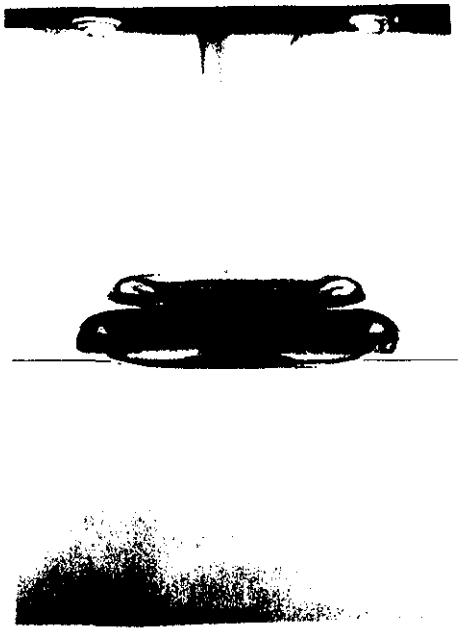

3d.

Figure 3. Comparison of two ring cases with vortex strength = 1.20. 3a. and 3b. have Γ = 38.1 cm^2/s, s.g.= 1.028; 3c. and 3d. have Γ = 22.2cm^2/s, s.g. = 1.01.

4a.

4c.

4b.

4d.

Figure 4. Comparison of two ring cases with vortex strength = 0.025. 4a. and 4b. have Γ = 107cm^2/s, s.g.= 1.005, done by LIF; 4c. and 4d. have Γ = 154cm^2/s, s.g. = 1.01.

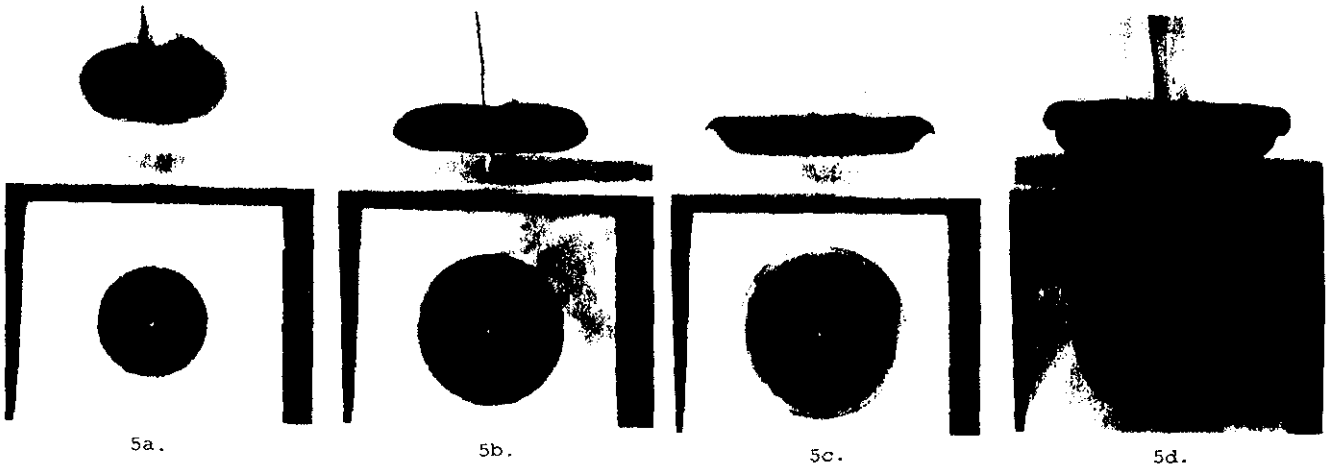

5a. 5b. 5c. 5d.

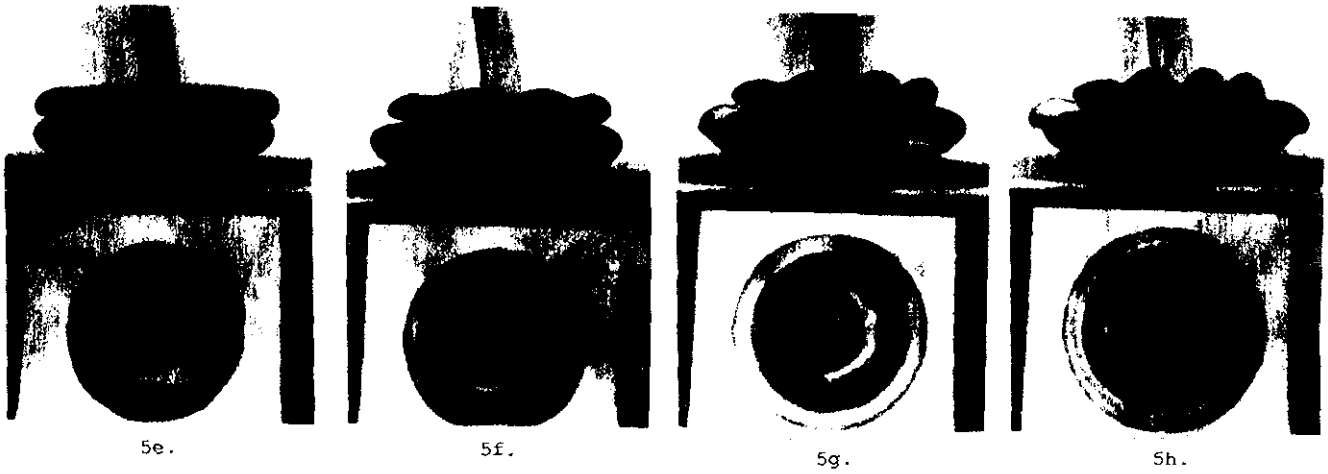

5e. 5f. 5g. 5h.

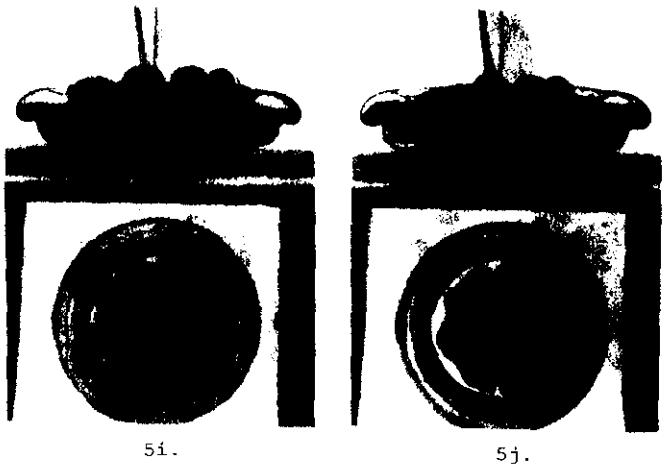

5i. 5j.

Figure 5. Vortex ring hitting a solid wall.

6a.

6b.

6c.

6d.

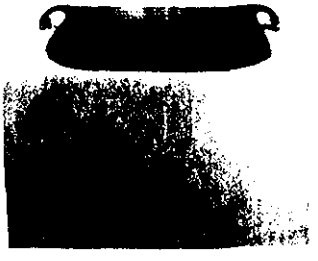

6e.

6f.

6g.

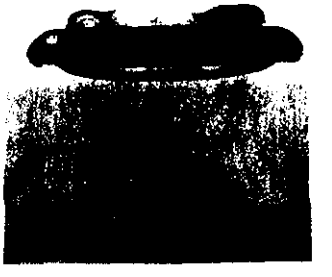

6h.

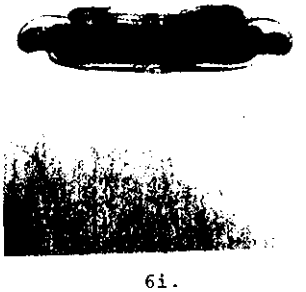

6i.

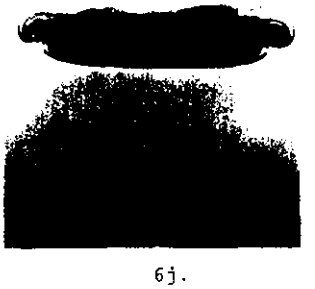

6j.

Figure 6. Weak ring/strong interface case; vortex strength = 1.20.

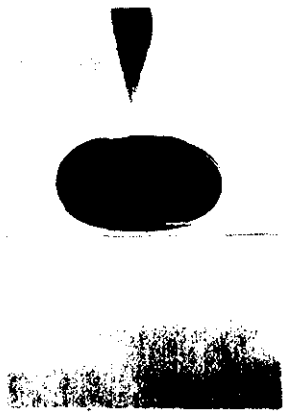

7a.

7b.

7c.

7d.

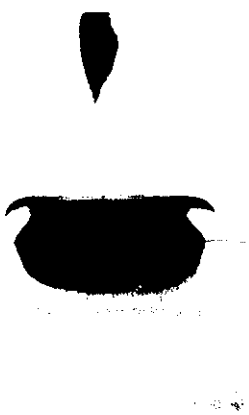

7e.

7f.

7g.

7h.

7i.

7j.

Figure 7. Intermediate case; vortex strength = 0.107.

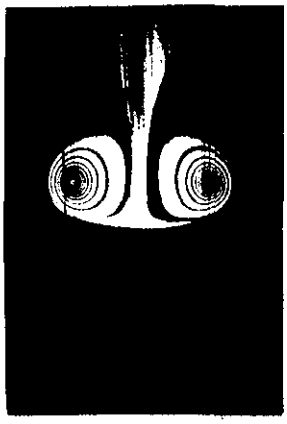

8a.

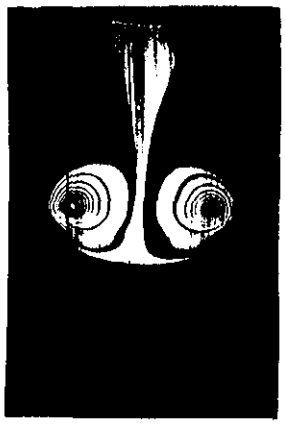

8b.

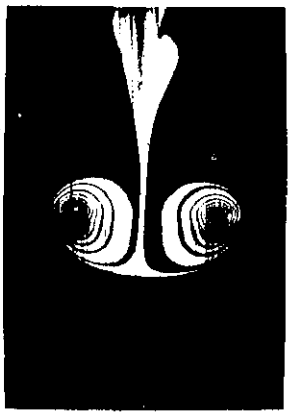

8c.

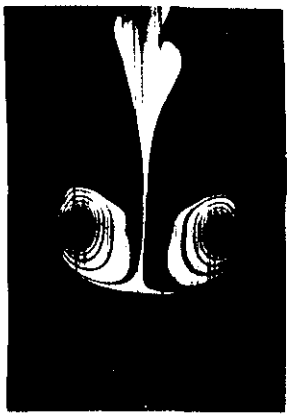

8d.

8e.

8f.

8g.

8h.

8i.

8j.

Figure 8. Strong ring/weak interface case; vortex strength = 0.025; ring visualized by LIF.